

Electron Paramagnetic Resonance Spectroscopic Study on Nonequilibrium Reaction Pathways in the Photolysis of Solid Nitromethane (CH₃NO₂) and D3-Nitromethane (CD₃NO₂)

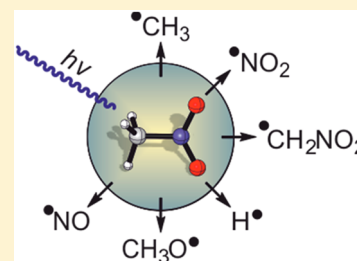
Yetsedaw Andargie Tsegaw and Wolfram Sander*

Lehrstuhl für Organische Chemie II, Ruhr-Universität Bochum, 44801 Bochum, Germany

Ralf I. Kaiser*

Department of Chemistry, University of Hawaii at Manoa, Honolulu, Hawaii 96822, United States

ABSTRACT: Thin films of nitromethane (CH₃NO₂) along with its isotopically labeled counterpart D3-nitromethane (CD₃NO₂) were photolyzed at discrete wavelength between 266 nm (4.7 eV) and 121 nm (10.2 eV) to explore the underlying mechanisms involved in the decomposition of model compounds of energetic materials in the condensed phase at 5 K. The chemical modifications of the ices were traced in situ via electron paramagnetic resonance, thus focusing on the detection of (hitherto elusive) reaction intermediates and products with unpaired electrons. These studies revealed the formation of two carbon-centered radicals [methyl (CH₃·), nitromethyl (CH₂NO₂·)], one oxygen-centered radical [methoxy (CH₃O·)], two nitrogen-centered radicals [nitrogen monoxide (NO·), nitrogen dioxide (NO₂·)], as well as atomic hydrogen (H·). The decomposition products of these channels and the carbon-centered nitromethyl (CH₂NO₂·) radical in particular represent crucial reaction intermediates leading via sequential molecular mass growth processes in the exposed nitromethane samples to complex organic molecules as predicted previously by dynamics calculations. The detection of the nitromethyl (CH₂NO₂·) radical along with atomic hydrogen (H·) demonstrated the existence of a high-energy decomposition pathway, which is closed under collisionless conditions in the gas phase.



1. INTRODUCTION

During the last decades, the nitromethane molecule (CH₃NO₂), the simplest representative of an organic nitro compound carrying a resonance stabilized functional group (nitro), has received considerable attention from the material science community because nitromethane is considered as a model compound of nitrohydrocarbon-based (RNO₂) energetic materials covering propellants,^{1,2} explosives,^{3–6} and high-performance fuel additives for internal combustion engines and detonation systems.⁷ A detailed knowledge of the underlying reaction mechanisms in the decomposition of nitromethane and of the successive reactions of the carbon-, nitrogen-, and oxygen-centered radicals formed in this process is imperative to predict the aging behavior, performance, and the sensitivity to heat and shock of energetic materials.^{8–15} The investigation of these decomposition processes still represents a significant hurdle for experimentalists, theoreticians, and modelers considering the nonequilibrium conditions under which these reactions often occur.

Previously, experimental investigation of the decomposition pathways of nitromethane has been mainly restricted to gas-phase processes utilizing ultraviolet photodissociation (UVPD)^{16–20} and infrared multiphoton dissociation (IRMPD).^{21–23} These studies were often conducted under collisionless conditions in molecular beams. Combined with electronic structure calculations, three key channels were

exposed: (1) the unimolecular decomposition of nitromethane (CH₃NO₂) to the methyl radical (·CH₃) and nitrogen dioxide (·NO₂) (reaction 1) and (2) a roaming-mediated nitromethane (CH₃NO₂)–methyl nitrite (CH₃ONO) isomerization followed by fragmentation of the methyl nitrite through a radical pathway to the methoxy radical (CH₃O·) plus nitrogen monoxide (·NO) (reaction 2a) and via a molecular elimination pathway forming formaldehyde (H₂CO) plus nitrosylhydride (HNO) (reaction 2b; Scheme 1).^{21,24–29}



Until recently, only limited studies have been conducted in the condensed phase. Photolysis studies of liquid nitromethane and nitromethane ices at 77 K suggested a decomposition of nitromethane in analogy to reaction 1 forming the methyl radical (·CH₃) plus nitrogen dioxide (·NO₂).^{30,31} Follow-up studies revealed the isomerization of nitromethane (CH₃NO₂) to methyl nitrite (CH₃ONO); successive photolysis leads to the

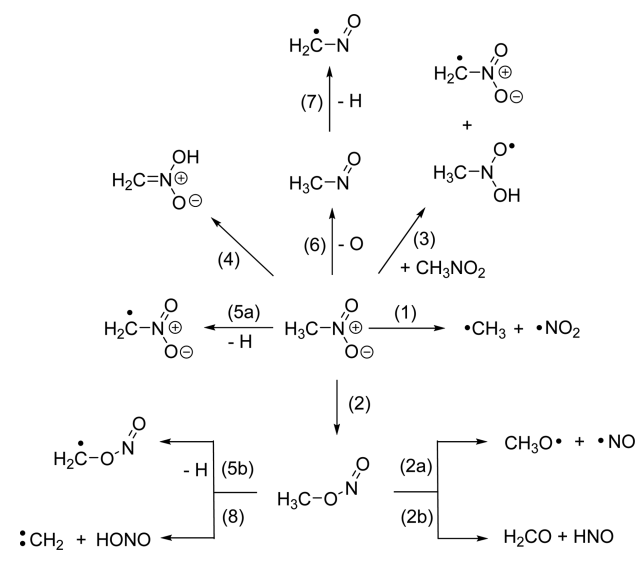
Received: December 22, 2015

Revised: February 9, 2016

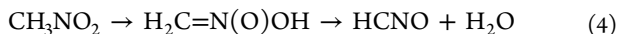
Published: February 10, 2016



Scheme 1. Compilation of Initial Isomerization and Decomposition Mechanisms of Nitromethane (CH₃NO₂) Inferred from Gas-Phase and Condensed-Phase Experimental Studies along with Molecular Dynamics Simulations (See Text for Details)

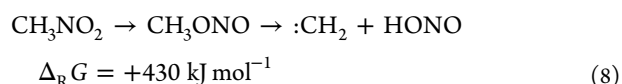
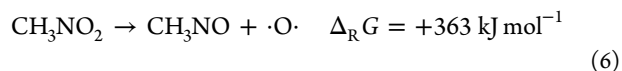
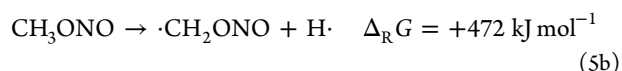
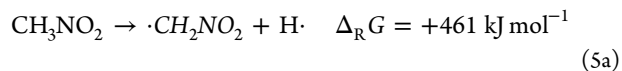


detection of the molecular fragmentation pathway to formaldehyde (H₂CO) and nitrosylhydride (HNO) (reaction 2b) and also a poorly understood isomerization to nitrosomethanol (ONCH₂OH).^{32–35} Extensive molecular dynamics simulations proposed that besides the traditional nitromethane (CH₃NO₂)-to-methylnitrite (CH₃ONO) isomerization, intermolecular hydrogen atom transfer processes yield *N*-hydroxy-nitrosomethane (CH₃N(O)·OH) plus a nitromethyl (·CH₂NO₂) radical (reaction 3) along with an isomerization to acinitromethane (H₂C=N(O)OH) (reaction 4).^{36,37} These computations revealed further that the decomposition of nitromethane should lead to a complex mixture of carbon-, oxygen-, nitrogen-, and hydrogen-bearing organics of hitherto unknown composition.^{36–38}



Recent experimental studies on the interaction of cryogenic films of nitromethane (CH₃NO₂) and of D3-nitromethane (CD₃NO₂) films with ionizing radiation in the form of energetic electrons and photons (Lyman α ; 10.2 eV) exposed that besides the classical gas-phase pathways (reactions 1 and 2), nitromethane (CH₃NO₂) follows high-energy (nonequilibrium) and strongly endoergic decomposition routes (reactions 5–8).^{39–41} As confirmed via isotopic substitution experiments, these involve the decomposition of nitromethane and/or the methylnitrite isomer to the nitromethyl radical (·CH₂NO₂) and/or methylene nitrite radical (·CH₂ONO) plus suprathermal atomic hydrogen (H·) (reactions 5a and 5b), to nitrosomethane (CH₃NO) plus atomic oxygen (·O) (reaction 6), to the nitrosomethyl radical (·CH₂NO) plus atomic hydrogen (H·) (reaction 7), and to singlet carbene (:CH₂) plus nitrous acid (HONO) (reaction 8). The carbon-centered radicals and closed-shell species indicated in italics in reactions 5a–8 were found to initiate mass growth processes leading to three key classes of complex organic molecules:^{39–41} (1) a homologues series of nitrosoalkanes [nitrosoethane (C₂H₅NO)

and nitrosopropane (C₃H₇NO)], (2) a homologues series of nitritoalkanes [ethylnitrite (C₂H₅ONO) and propylnitrite (C₃H₇ONO)], and (3) complex organics formally incorporating two nitromethane building blocks (CH₃NONOCH₃, CH₃NO-NO₂CH₃, CH₃OCH₂NO₂, and ONCH₂CH₂NO₂).



These pathways have been derived based on exposing mixed nitromethane–D3-nitromethane ices to ionizing radiation, following the chemical evolution of the irradiated ices on line and in situ via infrared spectroscopy, and subliming the newly formed molecules via temperature-programmed desorption followed by photoionizing the subliming molecules and detecting the latter via reflectron time-of-flight mass spectrometry (ReTOF).

Whereas the closed-shell species such as the nitrosoalkanes and nitritoalkanes were nicely identified via ReTOF and correlating shift of the mass-to-charge ratios of the products upon (partial) deuteration, the inferred carbon- and oxygen-centered radical intermediates and the atoms (hydrogen, oxygen) have not been identified, neither via infrared nor mass spectroscopic detection schemes, in our previous studies. This is due to the small amount of the radicals formed, their high reactivity, and/or the overlapping absorptions with the fundamentals of the corresponding closed-shell precursors. Consequently, a further analysis on the decomposition of nitromethane is absolutely critical to understand the full complexity of the process. Here, we provide the final pieces of the puzzle and attempt to identify multiple carbon-, oxygen-, and nitrogen-centered radicals formed in the wavelength-selective photolysis of solid nitromethane and D3-nitromethane, i.e., 266 nm (4.7 eV), 254 nm (4.9 eV), and 121 nm (10.2 eV) at 5 K exploiting electron paramagnetic resonance (EPR). Due to the closed-shell nature of the reactants, but the presence of unpaired electrons in the radical/atom intermediates, EPR provides essentially a “background free” detection method, thus providing unprecedented information on the formation and potential branching ratios of the open-shell products formed. We discuss these findings in the context of previous EPR studies of nitromethane exposed to ionizing radiation and then merge these novel data with those obtained from our previous FTIR and ReTOF analyses to ultimately reveal a unified picture of the decomposition of nitromethane in the condensed phase at ultralow temperatures.

2. EXPERIMENTAL SECTION

2.1. Materials and Methods. Nitromethane (99%+, Acros) and D3-nitromethane (99.5 atom % D+, abcr GmbH) were used in the experiments without further purification. For the matrix isolation experiments, argon and neon (Messer-Griessheim; 99.9999%) were exploited. X-band EPR experi-

ments were recorded with a Bruker Elexsys E500 EPR spectrometer holding an Er077R magnet with a 75 mm pole cap distance, an Er047XG-T microwave bridge, and an oxygen-free high-conductivity copper rod (75 mm length, 3 mm diameter) cooled by a Sumitomo SHI-4-5 closed-cycle 4.2 K cryostat.⁴²

2.2. EPR Measurements. Argon or neon matrices doped with 0.2–0.05% of nitromethane or D3-nitromethane were deposited on the copper rod, which was maintained at 5 K by a helium closed-cycle cryostat. Typically, deposition times range between 5 and 40 min. The copper rod was then lowered into a quartz tube (75 mm length, 10 mm diameter) at the bottom of the shroud, which allowed the matrix-isolated nitromethane (D3-nitromethane) to be irradiated at 254 nm (4.9 eV) from a low-pressure mercury lamp, 266 nm (4.7 eV) from a Nd:YAG laser, and 121 nm (10.2 eV) from a hydrogen-discharged lamp photons. Spectra were recorded at various irradiation times as detailed below.

2.3. EPR Simulations. The EPR spectra were simulated exploiting the EasySpin suite, a comprehensive software package for spectral simulation and analysis in EPR (version 5.0.2).⁴³ For the simulation, the experimental parameters including the frequency, number of points, and the spectral range were matched with those from the experiment; the dynamic parameters such as the Lorentzian line width and the distribution in magnetic parameters (g and A strains) were taken from literature data and adjusted to our frequency. Branching ratios are calculated by integration of the individual peaks of the radicals.

3. RESULTS

The photolysis of nitromethane (CH_3NO_2) and D3-nitromethane (CD_3NO_2) in both argon and neon matrices as well as in the pure solid at 5 K resulted in the appearance of multiple new features in the electron paramagnetic resonance spectrum (Figure 1). To assign these features, we pursue the following strategy. First, we simulate the EPR spectrum of each of the individual carbon-, nitrogen-, and oxygen-centered radicals predicted to be formed during the photolysis.^{39,41} Second, we exploit a linear combination of these individual spectra as base functions to simulate the experimentally obtained EPR spectra after the photolysis. Figure 1 demonstrates that distinct matrices in the experiments have little effect on the newly identified species; as expected, the peaks were found to be sharper in the matrix-isolated samples (Figure 1a). Also as can be seen in Figure 1a, no additional peaks emerge after about 20 min of irradiation; only the yield is enhanced. Finally, an annealing of the irradiated samples to 30 K decreases the intensity of the (radical) peaks as the result of radical diffusion and hence recombination (Figure 1b).

3.1. Individual EPR Spectra. **3.1.1. Methyl (CH_3) and D3-Methyl (CD_3) Radicals.** The EPR spectrum of the methyl radical (CH_3) consists of four lines (Figure 2a), which are observed after short irradiation times of about 1 min of nitromethane (CH_3NO_2) at 5 K. Because the unpaired electron is localized at the carbon atom, which is surrounded by three chemically equivalent hydrogen atoms, we expect a quartet of lines for the methyl (CH_3) radical as a result of the hyperfine interactions between the spin of the electron and the nuclear spin of three protons ^1H ($I = 1/2$). Similarly, we predict septet lines for the D3-methyl radical (CD_3) due to interaction of the unpaired electron with the three adjacent deuterium atoms ^2H ($I = 1$). The methyl radical trapped in low-temperature

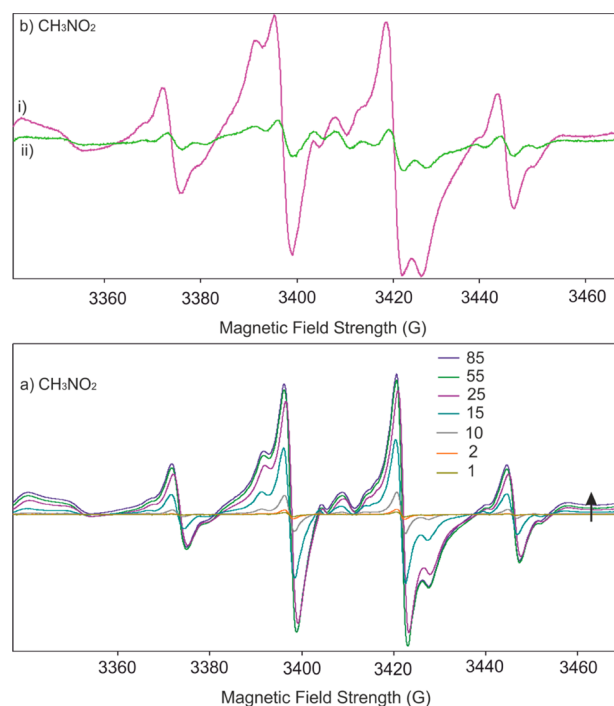


Figure 1. EPR spectra obtained after $\lambda = 254$ nm (4.9 eV) photolysis of matrix-isolated and neat nitromethane at 5 K: (a) 0.2% nitromethane (CH_3NO_2) in solid argon after irradiation times of 1, 2, 10, 15, 25, 55, and 85 min; (b) neat nitromethane (CH_3NO_2) after 180 min irradiation (i) and subsequent annealing at 30 K for 5 min (ii).

matrices have been studied by EPR spectroscopy previously; thus, the EPR parameters are already known.^{44–51} It was shown that at 4.2 K, the methyl radical has four EPR lines with a hyperfine coupling constant (hfcc) of an average of about 23.1 G. In agreement with these studies, our experiment at 5 K yields well-resolved and separated quartet lines attributed to the methyl radical with hfcc values of 23.06, 23.12, and 23.27 G (Figure 2a). Bielski et al. reported that the total separation of the four lines of the methyl radical formed after photolysis of nitromethane in a water matrix or a tetrachloride matrix at 77 K was 65 G, in close agreement to our experimental findings of 69.45 G.³⁰ The EPR parameters of the D3-methyl radical trapped in low-temperature matrices were also reported.^{44–46} It shows a septet of lines with an average hfcc of about 3.59 G. In our experiments we measured an average hfcc of 3.8 G septet lines for the D3-methyl radical (CD_3).⁴⁴

3.1.2. Nitromethyl (CH_2NO_2) and D2-Nitromethyl (CD_2NO_2) Radicals. In the case of the nitromethyl radical (CH_2NO_2), the unpaired electron is localized at the carbon atom. Because of coupling between the spin of the electron and the nuclear spin of the two adjacent protons ^1H ($I = 1/2$) as well as the nitrogen atom ^{14}N ($I = 1$), we expect to see a triplet of triplet EPR lines for the CH_2NO_2 radical (Figure 3a). The simulation enables us to extract the spin Hamiltonian parameters of CH_2NO_2 : the hfccs of the hydrogen atoms ($A_{\text{H}} = 23.19$ G) and the nitrogen atom ($A_{\text{N}} = 4.3$ G) and the g -value $g_{\text{iso}} = 2.0020$. This was found to be in close agreement to the reported values of $A_1(^1\text{H}) = 22$ G, $A_2(^1\text{H}) = 22$ G, $A_3(^{14}\text{N}) = 6$ G.^{52–54}

Similarly, we expect a quintet of triplets for the D2-nitromethyl (CD_2NO_2) radical. The two chemically equivalent deuterium atoms ^2H ($I = 1$) result in 5 lines, of which each

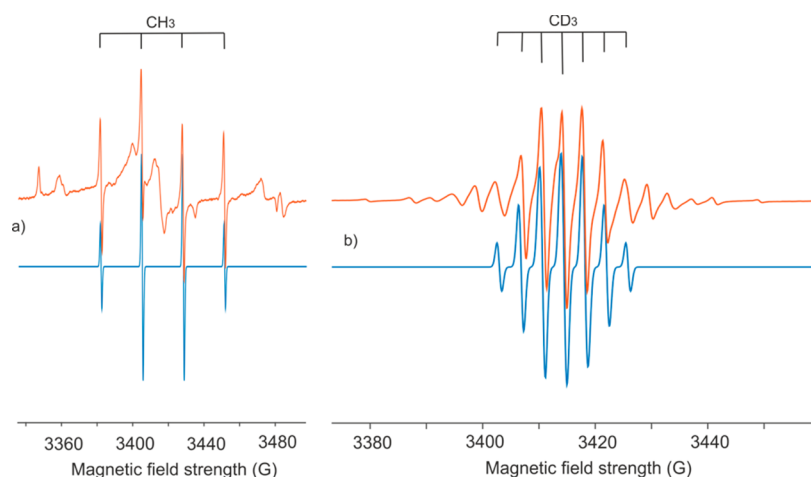


Figure 2. EPR spectra of methyl (a) and D3-methyl (b) radicals produced by $\lambda = 254$ nm (4.9 eV) irradiation of nitromethane (CH_3NO_2) and D3-nitromethane (CD_3NO_2), respectively, matrix isolated in argon (0.05%) at 5 K followed by annealing to 30 K for 5 min (red). The simulated spectra of the CH_3 and CD_3 radical are shown in blue with the simulation parameters compiled in Table 1.

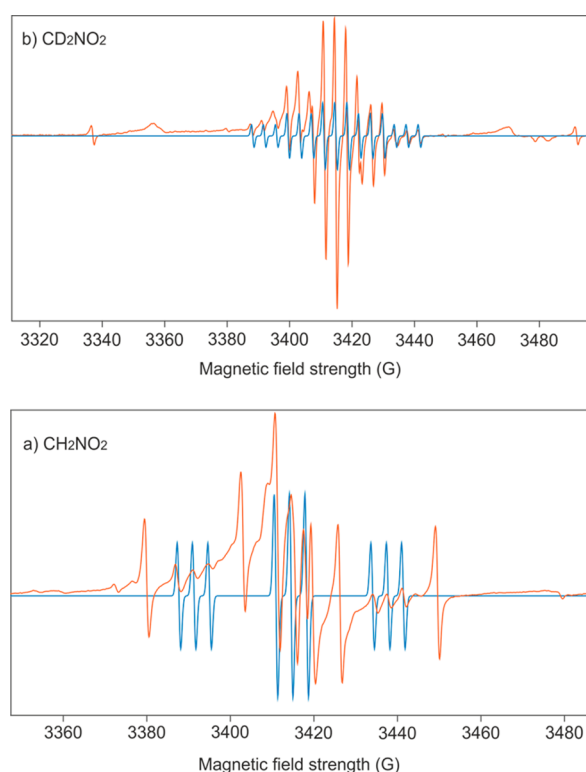


Figure 3. EPR spectra of nitromethyl (CH_2NO_2) (a) and D2-nitromethyl (CD_2NO_2) (b) produced by $\lambda = 266$ nm (4.7 eV) irradiation of nitromethane (CH_3NO_2) (doped with CD_3NO_2) and D3-nitromethane (CD_3NO_2) (doped with CH_3NO_2), respectively, matrix isolated in argon (0.05%) at 5 K. Simulated spectra of the CH_2NO_2 and CD_2NO_2 radical are shown in blue; experimental spectra of the individual radicals are depicted in red. The simulation parameters are given in Table 2.

component will then further split into three lines due to coupling with ^{14}N of the nitrogen dioxide nitrogen atom ($I = 1$) to give a total of $5 \times 3 = 15$ lines. The simulation of the experimental spectrum of CD_2NO_2 fits best with the following parameters: $A_1(^2\text{H}) = 11.4$ G, $A_2(^2\text{H}) = 11.4$ G, $A_3(^{14}\text{N}) = 3.85$ G, $g_{\text{iso}} = 2.0010$ (Figure 3b).

3.1.3. Methylene Nitrite (CH_2ONO) and D2-Methylene Nitrite (CD_2ONO) Radicals. The EPR spectrum of the methylene nitrite (CH_2ONO) radical was not yet reported. However, if the same rules apply to the nitromethyl radical (CH_2NO_2), i.e., we consider only the contribution of the Fermi contact term to the hyperfine structure and we take into account that the two protons are equivalent, we would expect to see $3 \times 6 = 18$ lines for the methylene nitrite radical. Similarly, a minimum of $5 \times 6 = 30$ lines are expected for D2-methylene nitrite radical. Neither 18 nor 30 unidentified lines are observed in the present experiments, indicating that (D2) methylene nitrite radicals are not formed or are below the detection limit of our system.

3.1.4. Nitrosomethyl (CH_2NO) and D2-Nitrosomethyl (CD_2NO) Radicals. The nitrosomethyl radical (CH_2NO) has not been studied in depth via EPR spectroscopy. Farmer and co-workers⁵⁵ reported the only experimental EPR studies of this radical in an argon matrix at 4 K. Very recently, Jaszewski et al.⁵⁶ carried out ab initio calculations of the EPR parameters of the nitrosomethyl radical (CH_2NO), which showed good agreement to earlier experimental findings of Farmer and co-workers. These authors suggested that the unpaired electron centered at the carbon atom couples to the ^{14}N nitrogen atom and also the two inequivalent hydrogen atoms located in *cis* and *trans* positions relative to the nonbonding electron pair of the nitrogen atom; this results in a complex, multiple-line spectrum of the nitrosomethyl radical (CH_2NO). The parameters reported were g -factors of $g_1 = 1.9930$, $g_2 = 2.0021$, and $g_3 = 2.0042$ along with hyperfine splitting of $A_1(^{14}\text{N}) = 33.7$ G, $A_2(^1\text{H}) = 26.2$ G and $A_3(^1\text{H}) = 2.8$ G. Using these parameters, the simulated spectrum of the nitrosomethyl radical (CH_2NO) is given in Figure 4. Also the EPR spectrum of D2-nitrosomethyl radical was not yet reported. By taking into account the difference in magnetic moment between the proton and deuteron, we similarly carried out simulation for the CD_2NO radical. However, in the present experiment, both CH_2NO and CD_2NO radicals remain unobserved.

3.1.5. Methoxy (CH_3O) and D3-Methoxy (CD_3O) Radicals. The EPR spectrum of the methoxy radical (CH_3O) formed upon photolysis of nitromethane in a perfluoromethylcyclohexane matrix at 77 K is documented.⁵⁷ The reported parameters are as follows: hyperfine coupling constant ($A^1\text{H}$)

Table 1. EPR Parameters of Methyl (CH_3) and D3-Methyl (CD_3) Radicals at 5 K

sample	temp (K)	g-values			hyperfine coupling constant (hfcc) (G)				ref
		g_1	g_2	g_3	A_1	A_2	A_3	A_{iso}	
H_2+CO	4.2	2.0026	2.0026	2.0022	23.50	23.50	22.20	23.07	50
D_2+CO	4.2	2.0026	2.0026	2.0022	3.62	3.62	3.42	3.55	50
CH_4	4.1	–	–	–	23.00	23.15	23.33	23.15	44
CH_3NO_2	5.0	2.0005	2.0005	2.0005	23.06	23.12	23.27	23.15	this work
CD_3NO_2	5.0	2.0007	2.0008	2.0009	3.73	3.84	3.84	3.80	this work

Table 2. EPR Parameters of Nitromethyl (CH_2NO_2) and D2-Nitromethyl (CD_2NO_2) Radicals

sample	temp (K)	g-values			hyperfine coupling constant (hfcc) (G)			ref
		g_1	g_2	g_3	A_1	A_2	A_3	
CH_3NO_2	5	2.0020	2.0020	2.0020	23.19	23.19	4.30	this work
CH_3NO_2	77	–	–	–	22	22	5	52
CD_3NO_2	5	2.0010	2.0010	2.0010	11.4	11.4	3.85	this work

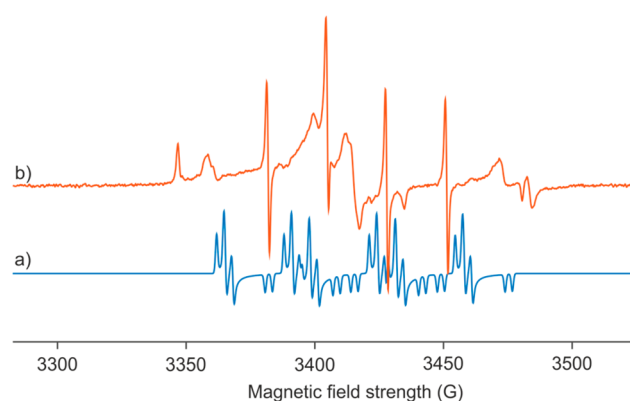


Figure 4. (a) Simulated spectra of the nitrosomethyl radical (CH_2NO); (b) EPR spectrum produced by $\lambda = 254$ nm (4.9 eV) irradiation of nitromethane (CH_3NO_2), matrix isolated in argon (0.05%), over 18 h at 5 K, followed by annealing at 30 K for 5 min.

is 9 G and g -factors are 2.0135 (perpendicular) and 1.9932 (parallel). These data are in excellent agreement with our simulations proposing a best fit to the experimental spectrum ($A^{\text{H}} = 9$ G and g -factors $g_1 = 2.0122$, $g_2 = 1.9934$, and $g_3 = 2.0315$ (Figure 5). However, we failed to detect the D3-

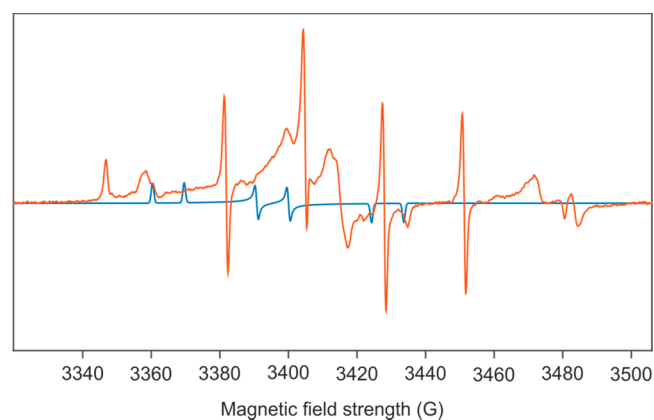


Figure 5. Comparison of simulated spectrum of the methoxy (CH_3O) radical (blue) with the EPR spectrum of the methoxy radical produced by $\lambda = 254$ nm (4.9 eV) irradiation of nitromethane (CH_3NO_2) for 18 h, matrix isolated in argon (0.05%) at 5 K followed by annealing at 30 K for 5 min (red).

methoxy radical (CD_3O) upon photolysis of D3-nitromethane; this is likely due to the overlap with the spectral lines of the CD_2NO_2 and CD_3 photoproducts.

3.1.6. Nitrogen Dioxide (NO_2). We expect three EPR lines ($M_1 = +1, 0, -1$) for nitrogen dioxide (NO_2), which result from the interaction of the unpaired electron with the nuclear spin of the nitrogen atom ^{14}N ($I = 1$). In addition, in a randomly oriented nitrogen dioxide (NO_2) molecule, each M_1 value will split further into three x , y , and z components to give a total of $3 \times 3 = 9$ lines.^{58,59} Experimentally, the EPR spectrum of nitrogen dioxide (NO_2) in low-temperature matrices has been extensively investigated.^{58,60–65} It was shown that the spectral line shapes as well as line positions of the nitrogen dioxide (NO_2) are temperature-dependent. Thus, the value of the hfcc due to the interaction of the magnetic moment of the unpaired electron with the nitrogen atom varies from about 55 G at 4 K to 12 G at 173 K, of average splitting of the triplet spectrum observed for nitrogen dioxide (NO_2).⁶¹ It was also reported that the rotational motion of the nitrogen dioxide (NO_2) radical is axially symmetric about the y axis (parallel to O–O bond direction; Figure 6) over the temperature range from 12 to 87 K.^{60,62,64} Therefore, even at the low temperature of 4 K, the x and z components of the g and A tensors of nitrogen dioxide are less resolved, whereas the y components are observable up to 102 K.⁶⁰ In accordance to these studies, we observed in the present experiments well-resolved y -components of the nitrogen dioxide (NO_2) radical at 5 K (Figure 6).

The spin Hamiltonian parameters (the g and A tensor components) for nitrogen dioxide (NO_2) in various selected matrices over a wide range of temperatures are summarized in Table 3. The values reported in the literature were found to be in good agreement with our experimental results. Our simulation best fit to the experimental spectrum of nitrogen dioxide (NO_2) produced by irradiation of nitromethane using the parameters $g_x = 2.0026$, $g_y = 1.9907$, $g_z = 2.0025$, $A_x = 51.0$ G, $A_y = 43.7$ G, $A_z = 67.9$ G, and $A_{\text{iso}} = 54.4$ (Table 3, row 1) at 5 K; the parameters were slightly changed when the matrix was annealed between 20 and 30 K ($g_x = 2.0009$, $g_y = 1.9892$, $g_z = 2.0010$, $A_x = 56.5$ G, $A_y = 44.6$ G, $A_z = 68.5$ G, and $A_{\text{iso}} = 56.5$ (Table 3).

Bielski et al. reported two triplet lines for the NO_2 radical: one major triplet with an average separation of 58 G and one minor triplet with a 46 G separation, giving a total of $3 + 3 = 6$ lines in the EPR spectrum which were observed upon photolysis of nitromethane at 77 K.³⁰ This is in agreement

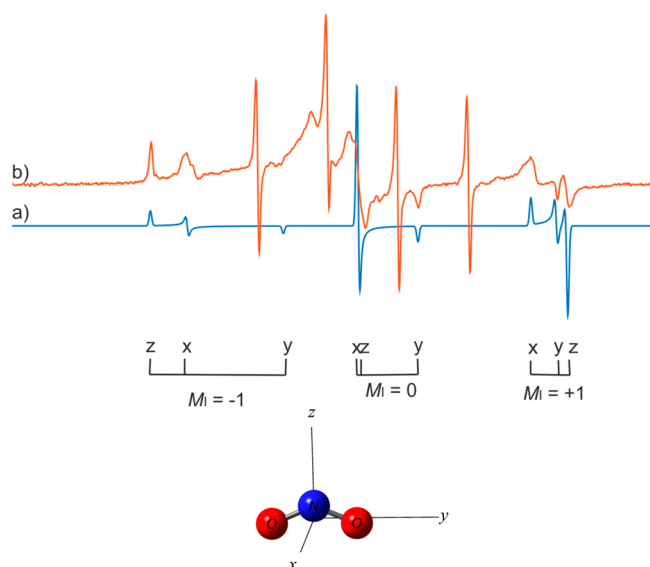


Figure 6. (a) Simulated spectrum of nitrogen dioxide (NO_2) and (b) the EPR spectrum produced by $\lambda = 254$ nm (4.9 eV) irradiation of nitromethane (CH_3NO_2) for 18 h matrix isolated in argon (0.05%) at 5 K followed by annealing to 30 K for 5 min. The simulation parameters are given in Table 3.

with our experimental results at 5 K: $A_y = 46$ G and an average A_x and A_z of 57.5 G. The fact that we have got a well-resolved and separated triplet of triplets in the spectrum of nitrogen dioxide (NO_2) upon photolysis of nitromethane could be explained by the difference in temperature and the use of argon matrices in our experiments. While we used inert gas matrices at 5 K in the present experiments, previous experiments exploited water and carbon tetrachloride matrices at 77 K.³⁰

3.1.7. Nitrogen Monoxide (NO). The EPR spectrum of nitrogen monoxide (NO) has been reported previously.^{67–72} The coupling between the unpaired electron and the nitrogen atom results in spin Hamiltonian parameters of $g_1 = 2.008$, $g_2 = 2.0061$, $g_3 = 2.0027$, $A_1 = 5.7$ G, $A_2 = 5.7$ G, $A_3 = 30.7$ G, and $A_{\text{iso}} = 14.1$ G.⁶⁷ These are in a close agreement with our best fit simulations of the nitrogen monoxide (NO) radical with the parameters $g_1 = 2.0027$, $g_2 = 2.0064$, $g_3 = 2.0002$, $A_1 = 6.4$ G, $A_2 = 3.6$ G, $A_3 = 30.7$ G, and $A_{\text{iso}} = 13.6$ (Figure 7, Table 4).

3.1.8. Atomic Oxygen (O). Among the three naturally occurring isotopes of oxygen, ^{16}O and ^{18}O have a nuclear spin of $I = 0$; hence, we do not expect any magnetic hyperfine structure. In contrast, the least abundant isotope, ^{17}O , has a

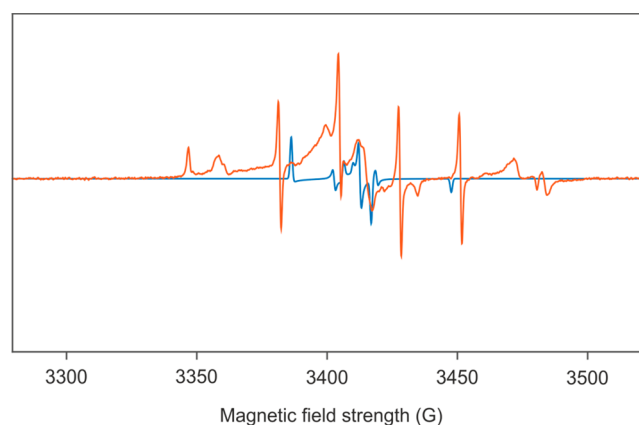


Figure 7. Comparison of (a) simulated spectrum of nitrogen monoxide radical (NO) (b) with the EPR spectrum of the nitrogen monoxide (NO) radical produced by $\lambda = 254$ nm (4.9 eV) irradiation of nitromethane (CH_3NO_2) for 18 h, matrix isolated in argon (0.05%) at 5 K followed by annealing to 30 K for 5 min.

Table 4. EPR Parameters of the Nitrogen Monoxide (NO) Radical

g-values			hyperfine coupling constant (hfcc) / (G)				ref
g_1	g_2	g_3	A_1	A_2	A_3	A_{iso}	
2.0080	2.0061	2.0027	5.7	5.7	30.7	14.1	67
2.0027	2.0064	2.0002	6.4	3.6	30.7	13.6	this work

nuclear spin of $I = 5/2$. Thus, in theory we should get a sextet of lines in the corresponding EPR spectrum. However, on the basis of the abundances of the photoproducts in our experiments and the natural abundance of ^{17}O , we expect the yield of ^{17}O atoms in their ^3P electronic ground state to be below the level of detection. Here, it is well-known that atomic oxygen has a ^3P electronic ground state. Here, the spin orbit term of $j = 2$ results in a separation of 1.85 G and hence four lines ($M_I = 2 \rightarrow 1, 1 \rightarrow 0, 0 \rightarrow -1, -1 \rightarrow 1$); for $j = 1$, this results in a separation of 10.7 G and a doublet ($M_I = 1 \rightarrow 0, 0 \rightarrow -1$), i.e., a total of $4 + 2 = 6$ lines.^{73–75} Although we exploited a solid argon matrix at 5 K, we could not detect any signal of atomic oxygen. Using parameter hfcc values of $A = 15.1$ G and $g = 2.0023$ and nucleus ^{17}O , the simulation suggests this could probably be due to overlapping of the spectral lines with CH_3 , NO_2 , and NO radicals and the low-concentration oxygen atoms (Figure 8).

Table 3. EPR Parameters of Nitrogen Dioxide (NO_2) in Various Media

sample	temp (K)	g-values			hyperfine coupling constant (hfcc) (G)				ref
		g_x	g_y	g_z	A_x	A_y	A_z	A_{iso}	
CH_3NO_2	5	2.0026	1.9907	2.0025	51.5	43.7	67.9	54.4	this work
CH_3NO_2	30	2.0009	1.9892	2.0010	56.5	44.6	68.5	56.5	this work
CD_3NO_2	5	2.0026	1.9907	2.0025	51.5	43.7	67.9	54.4	this work
CD_3NO_2	30	2.0026	1.9900	2.0008	56.5	45.5	68.6	56.8	this work
CH_3NO_2	77	2.0060	1.9910	2.0020	47	46	66	53.0	54
vyacor ^a	4.8	2.0051	1.9913	2.0017	50	46	65.5	53.8	62
zeolite ^a	4.8	2.0051	1.9913	2.0017	50	46	65.5	53.8	62
SiO_2 ^a	4.2	2.0057	1.9920	2.0020	50.1	45.8	65.5	53.8	60
MgO ^a	77	2.005	2.002	1.9910	52	65	49	55.3	66

^a NO_2 adsorbed on surface studies



Figure 8. Comparison of (a) the simulated spectrum of atomic oxygen to (b) the EPR spectrum produced by $\lambda = 254$ nm (4.9 eV) irradiation of nitromethane (CH_3NO_2) matrix isolated in argon (0.05%) at 5 K followed by annealing to 30 K for 5 min.

3.1.9. Atomic Hydrogen (H) and Deuterium (D). The EPR parameters of atomic hydrogen trapped in low-temperature matrices are frequently reported in the literature.^{76–78} It was shown that below 70 K, atomic hydrogen has two spectral lines separated by about 510 G, centered at approximately $g = 2$ and $hfcc A = 504.9$ G. The $hfcc$ and g -factor of free hydrogen atom are also theoretically known to be 506.8 G and 2.0028384, respectively.^{78–81} These reports agreed well with our finding of two lines for atomic hydrogen produced by photolysis of nitromethane, which are separated by about 508 G, centered at $g = 2.002$ and described by $hfcc$ of (A^1H) = 505.62 G (Figures 9 and 10, Table 5). Similarly, upon decomposition of D3-

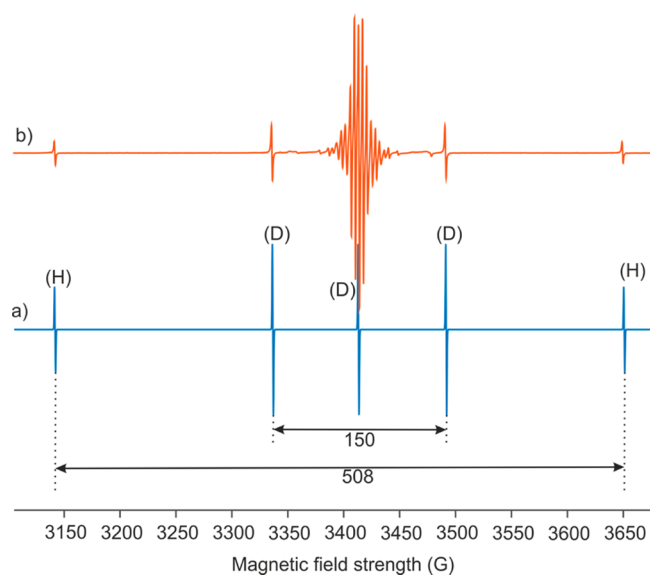


Figure 9. (a) Simulated spectrum of atomic hydrogen and deuterium shown in blue; (b) the individual EPR spectra of atomic hydrogen and deuterium (red) produced by $\lambda = 266$ nm (4.7 eV) laser irradiation of the mixture of excess D3-nitromethane (CD_3NO_2) and nitromethane (CH_3NO_2) for 30 min matrix isolated in argon (0.05%) at 5 K.

nitromethane, we observe three lines assigned to deuterium atoms which are separated by about 150 G with a g -factor of 2.007 and $hfcc$ of 77.43 G. These values agree well with the reported values of 150, 2.0023, and 77.88 G, respectively (Figure 9, Table 5).^{77,81}

3.2. Simulation of the Experimental EPR Spectra. We use a linear combination of the individual EPR spectra (sections 3.1.1–3.1.9.) to simulate the complex experimental EPR spectra of the photolysis products (Figures 11 and 12). The results are compiled in Table 6. The photolysis of (D3)-nitromethane ices at 266 nm (4.7 eV), 254 nm (4.9 eV), and 121 nm (10.2 eV) at 5 K excites the $\pi^* \leftarrow n$, $\pi^* \leftarrow \pi$, and $\pi^* \leftarrow \sigma$ transitions.^{82–85}

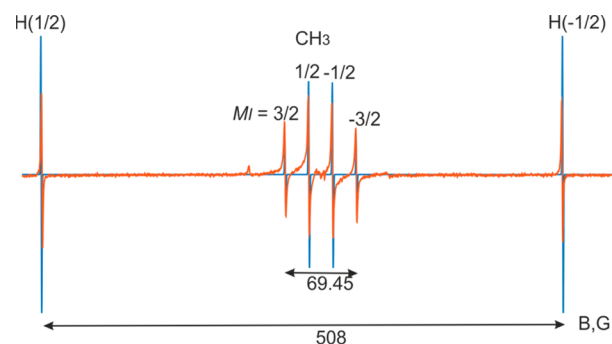


Figure 10. EPR spectra produced by $\lambda = 266$ nm (4.7 eV) irradiation of nitromethane (CH_3NO_2) for 10 min matrix isolated in argon (0.05%) at 5 K. The simulated spectra of the methyl (CH_3) radical and atomic hydrogen (H) shown in blue fit well with the experimental spectrum shown in red. Simulation parameters are given in Tables 1 and 5.

Table 5. EPR Parameters of Atomic Hydrogen (H) and Deuterium (D)

sample/radical	temp (K)	g -tensor	hyperfine coupling constant ($hfcc$) (G)	ref
free hydrogen atoms		2.0023	506.84	81
$\text{CH}_3\text{NO}_2/\text{H}$	5	2.0020	505.62	this work
$\text{C}_{32}\text{H}_{72}\text{O}_{12}\text{Si}_8/\text{H}$	10	2.0029	505.19	76
$(\text{OSi}(\text{CH}_3)_3)_8\text{Si}_8\text{O}_{12}/\text{H}$	40	–	506.06	77
free deuterium atoms		2.0023	77.88	81
$\text{CD}_3\text{NO}_2/\text{D}$	5	2.0070	77.43	this work
$(\text{OSi}(\text{CD}_3)_3)_8\text{Si}_8\text{O}_{12}/\text{D}$	40	–	77.87	77

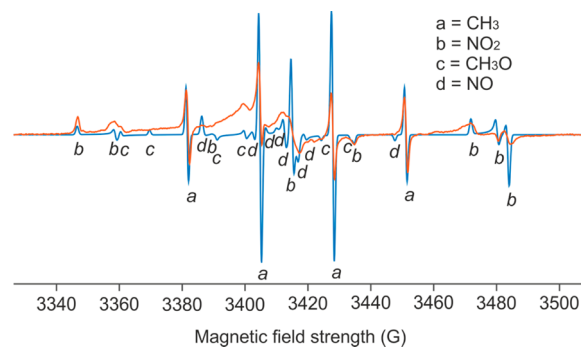


Figure 11. EPR spectra produced by $\lambda = 254$ nm (4.9 eV) irradiation of nitromethane (CH_3NO_2) over 18 h matrix isolated in argon (0.05%) at 5 K followed by annealing to 30 K for 5 min. The simulated spectra of the methyl (CH_3), nitrogen dioxide (NO_2), methoxy (CH_3O), and nitrogen monoxide (NO) radicals are shown in blue with the experimental spectrum overlaid in red.

In general, the radicals observed are not found to be wavelength-dependent with the exception that the (D2) nitromethyl radicals ($\text{CH}_2\text{NO}_2/\text{CD}_2\text{NO}_2$) radicals are obtained in higher yield while using 266 nm (4.7 eV) and 121.5 nm (10.2 eV) photons.

The (D3)-methyl radical (CH_3/CD_3) was detected at all three photolysis wavelengths in neat and also isotopically mixed ices. Similarly, hydrogen (H) and deuterium (D) could be monitored in all samples as well. The absorptions of these four species are prominent in the EPR spectra already after the first minute of photolysis at all wavelengths and contribute to the dominating EPR signal and account for up to $55 \pm 10\%$ ($\text{CH}_3/$

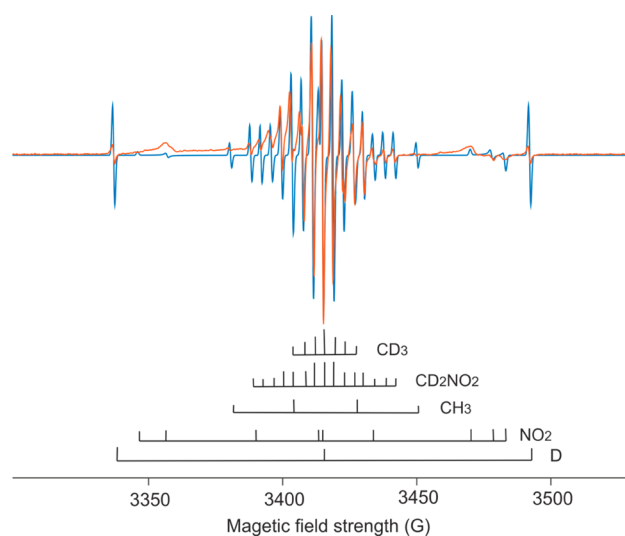


Figure 12. EPR spectra produced by $\lambda = 254$ nm (4.9 eV) irradiation of a mixture of D3-nitromethane (CD_3NO_2) and nitromethane (CH_3NO_2) for 18 h followed by annealing to 30 K for 5 min matrix isolated in argon (0.05%) at 5 K. The simulated spectra of D3-methyl (CD_3), D2-nitromethyl (CD_2NO_2), deuterium atoms (D), nitrogen dioxide (NO_2), and methyl (CH_3) radicals are shown in blue; the experimental spectrum is overlaid in red.

CD_3) and $30 \pm 10\%$ (H/D) of all open-shell products. Also, the nitrogen-centered radicals, nitrogen dioxide (NO_2) and nitrogen monoxide (NO), were identified upon photolysis of the low-temperature ices at all wavelengths. These species account for up to $15 \pm 5\%$ and $10 \pm 5\%$ of the open-shell reaction products, respectively. Furthermore, the oxygen-centered methoxy radical (CH_3O) could be verified to be formed upon photolysis of the nitromethane samples at all wavelengths at levels of up to $10 \pm 5\%$. Finally, the EPR studies provided compelling evidence of the formation of the (D2)-nitromethyl radical ($\text{CH}_2\text{NO}_2/\text{CD}_2\text{NO}_2$) at levels of up to $25 \pm 5\%$. We stress that despite extensive searches, we were unable to identify atomic oxygen (O), the methylene nitrite (CH_2ONO), or nitrosomethyl (CH_2NO) radicals in the irradiated ices. Based on the overlap with the EPR signal of

the photoproducts as compiled in Table 6, we can derive upper limits of 10%, 15%, and 15%, respectively.

4. DISCUSSION AND CONCLUSIONS

The present studies identified two carbon-centered radicals [methyl (CH_3) ($55 \pm 10\%$), nitromethyl (CH_2NO_2) ($25 \pm 5\%$)], one oxygen-centered radical [methoxy (CH_3O) ($10 \pm 5\%$)], two nitrogen-centered radicals [nitrogen monoxide (NO) ($10 \pm 5\%$), nitrogen dioxide (NO_2) ($15 \pm 5\%$)], as well as atomic hydrogen [H ($30 \pm 10\%$)] with the branching ratios given in parentheses; despite extensive searches, oxygen (O; $< 10\%$), the methylene nitrite (CH_2ONO ; $< 15\%$), and nitrosomethyl (CH_2NO ; $< 15\%$) could not be identified.

First, we compare our results with previous EPR investigations on the interaction of ionizing radiation with nitromethane (CH_3NO_2) in the condensed phase.^{30,52–54,57} These experiments revealed that the formation of methyl (CH_3), nitromethyl (CH_2NO_2), nitrogen dioxide (NO_2), and methoxy (CH_3O) radicals agrees well with our findings. Bielski et al. (1964) conducted an EPR experiment exploiting a mercury lamp photolysis of nitromethane in a water and a tetrachloride matrix at 77 K confirming the formation of both methyl (CH_3) and nitrogen dioxide (NO_2) radicals after short irradiation times.³⁰ With prolonged irradiation times, complex sets of multiplets appeared, which were tentatively attributed to nitrogen monoxide (NO) and methoxy (CH_3O) radicals. Chachaty (1965) carried out α -particle irradiation of nitromethane at 77 K; these showed the presence of methyl (CH_3), nitrogen dioxide (NO_2), and nitromethyl (CH_2NO_2) radicals.⁵³ The same group (1969) suggested that the photolysis of nitromethane in a perfluoromethylcyclohexane at 77 K produced mainly the methoxy (CH_3O) radical.⁵⁷ Finally, Symons (1988) exposed nitromethane and D3-nitromethane to ^{60}Co γ -rays at 77 K and observed mainly methyl (CH_3) and nitrogen dioxide (NO_2) radicals.⁵⁴

Based on these considerations, we discuss now the decomposition pathways of nitromethane (CH_3NO_2) upon photolysis. We note that none of the previous experiments^{30,52–54,57} was able to detect six radicals simultaneously. Furthermore, atomic hydrogen and nitrogen monoxide (NO) radical have never been observed as a photolysis product in

Table 6. Summary of Photolysis Experiments of Nitromethane and D3-Nitromethane in Various Media

sample	wavelength (nm) (eV)	irradiation time (min)	matrix	temp (K)	observed products
CH_3NO_2	254 (4.9)	1	Ar, Ne	5	CH_3 , H
		5	Ar, Ne	5	CH_3 , H, NO_2
		20	Ar, Ne	5	CH_3 , NO_2 , H, NO, CH_3O
		5	Ar, Ne	20–30 ^a	CH_3 , NO_2 , H, NO, CH_3O
	254 (4.9)	30	neat	5	CH_3 , NO_2 , H, NO, CH_3O
	266 (4.7)	20	Ar, Ne	5	CH_3 , NO_2 , H, NO, CH_3O , CH_2NO_2
	121.5 (10.2)	20	Ar	5	CH_3 , NO_2 , H, NO, CH_3O , CH_2NO_2
$\text{CH}_3\text{NO}_2 + \text{CD}_3\text{NO}_2$	254 (4.9)	20	Ar	5	CH_3 , CD_3 , NO_2 , H, D, CH_2NO_2 , CD_2NO_2
		5	Ar	20–30 ^a	CH_3 , CD_3 , NO_2 , CH_2NO_2 , CD_2NO_2 , H, D
	266 (4.7)	20	Ar	5	CH_3 , CD_3 , NO_2 , CH_2NO_2 , CD_2NO_2 , H, D
	121.5 (10.2)	20	Ar	5	CH_3 , CD_3 , NO_2 , CH_2NO_2 , CD_2NO_2 , H, D
CD_3NO_2	254 (4.9)	25	Ar, Ne	5	CD_3 , D, NO_2 , CD_2NO_2
		5	Ar	20–30 ^a	CD_3 , D, NO_2 , CD_2NO_2
	266 (4.7)	20	Ar	5	CD_3 , D, NO_2 , CD_2NO_2
	121.5 (10.2)	20	Ar	5	CD_3 , D, NO_2 , CD_2NO_2

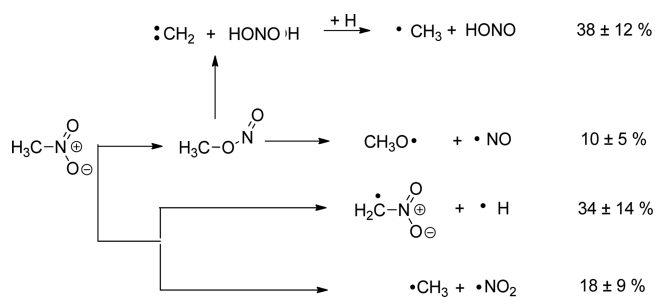
^aAfter 18 h of irradiation at 5 K, the matrix was annealed to 20–30 K for 5 min.

previous experiments. Finally, none of the aforementioned experiments^{30,52–54,57} attempted to quantify the branching ratios of the open-shell species produced. First, considering the decomposition pathways, it is important to highlight that both the methoxy (CH₃O) and the nitrogen monoxide (NO) radicals were detected with a branching ratio of 10 ± 5%. The observed 1:1 ratio agrees well with our previous findings^{39–41} that the methylnitrite molecule (CH₃ONO), formed via isomerization of nitromethane (CH₃NO₂), represents the common precursor to the methoxy (CH₃O) and the nitrogen monoxide (NO) radical (reaction 2a) upon exposure to ionizing radiation in the condensed phase; the competing pathway (reaction 2b), which was previously detected via infrared spectroscopy,^{39–41} cannot be probed via EPR spectroscopy in the present experiments because both products are closed-shell species and hence do not exhibit any absorptions in the EPR spectra. Second, within the experimental error limits, the nitromethyl radical (CH₂NO₂) (25 ± 5%) and atomic hydrogen [H (30 ± 10%)] were also quantified to be formed at a ratio of 1:1. Similar to the aforementioned discussion, photolysis of nitromethane (CH₃NO₂) via reaction 5a provides a rational decomposition pathway, which was previously proposed based on results of exposing isotopically mixed CH₃NO₂/CD₃NO₂ ices to ionizing radiation.⁴¹ This pathway was found not to be open in previous gas-phase studies conducted under single collision conditions (c.f. Introduction). Third, the potential decomposition of nitromethane (CH₃NO₂) to methyl (CH₃) (55 ± 10%) plus nitrogen dioxide (NO₂) (15 ± 5%) (reaction 1) has to be discussed. Recall that this pathway was observed in prior gas-phase studies conducted under single-collision conditions, but the lack of detection of the methyl radical (CH₃) in infrared spectra in previous studies of the nitromethane (CH₃NO₂) system exposed to ionizing radiation^{39–41} suggested that this channel was closed in the condensed phase at 5 K. A comparison of the experimentally determined branching ratio of methyl (CH₃) to nitrogen dioxide (NO₂) of 3.7 ± 1.5 versus the expected branching ratio of 1:1 (reaction 1) suggests that in the present experiments, almost two-thirds of the methyl radicals cannot be formed via decomposition of nitromethane (CH₃NO₂). Our studies propose that reaction 1 is open in the condensed phase upon photolysis of nitromethane (CH₃NO₂); considering the branching ratio of reaction 1 and accounting for the signal-to-noise of the previous infrared studies,^{39,40} methyl radicals are below the detection limit in the infrared spectra. Based on the branching ratios and the inherent stoichiometry of the decomposition products formed via reactions 1, 2a, and 5a, methyl radicals (CH₃) at levels of 30 ± 10% likely origin from another source. Considering the lower error limits of the branching ratios of the nitromethyl radical (CH₂NO₂) (25 ± 5%) and atomic hydrogen (H) (30 ± 10%), up to 20% of the intensity of the detected hydrogen atoms might not be accounted for. This value correlates nicely with the fraction of the hitherto unaccounted source of the methyl radicals (30 ± 10%), which once again proposes that a fraction of the methyl radicals might be the reaction products of atomic hydrogen (H) with hitherto unidentified reaction partner. Recall that the mass-growth products of previous low-temperature studies^{39–41} propose that the methylnitrite molecule (CH₃ONO) also decomposes via reaction 8, forming carbene (:CH₂) plus nitrous acid (HONO). Therefore, in the present experiments, carbene (:CH₂) might react with atomic hydrogen (H) to form the hitherto unaccounted fraction of the methyl radicals (CH₃).

Although it was also searched for, we were not successful in identifying triplet carbene in the present EPR studies. This could be due to the fact that rapid reactions with abundant atomic hydrogen convert carbene into methyl radicals.

In summary, we presented a comprehensive investigation on the photolysis of (D3)-nitromethane (CH₃NO₂) ices. These studies identified a comprehensive suite of radicals formed in these processes with the branching ratios compiled in parentheses: methyl (CH₃; 55 ± 10%), nitromethyl (CH₂NO₂; 25 ± 5%), methoxy (CH₃O; (10 ± 5%)), nitrogen monoxide (NO; 10 ± 5%), nitrogen dioxide (NO₂; 15 ± 5%), and atomic hydrogen (H; 30 ± 10%). A detailed analysis of the branching ratios of the open-shell species formed in these processes verified the existence of a nitromethane (CH₃NO₂)–methylnitrite (CH₃ONO) isomerization along with the four decomposition pathways; three channels (equations 1, 2a, and 5a) could be observed directly via the spectroscopically monitored products plus their branching ratios, whereas reaction 8 was inferred indirectly from the branching ratios and stoichiometry of the reaction products (Scheme 2). These

Scheme 2. Compilation of Isomerization and Decomposition Mechanisms of Nitromethane (CH₃NO₂) Inferred from the Present EPR Studies along with Overall Branching Ratios of the Four Pathways Identified



studies provide valuable insights into the underlying reaction mechanisms in the decomposition of nitromethane as a model compound of energetic materials to forecast the aging behavior, performance, and sensitivity to heat and shock of energetic materials.

AUTHOR INFORMATION

Notes

The authors declare no competing financial interest.

ACKNOWLEDGMENTS

This material is based on work supported by the U.S. Army Research Office under Grant W911NF-14-1-0167 (R.L.K.). The Bochum team (Y.A.T., W.S.) thanks the Cluster of Excellence RESOLV (EXC 1069) funded by the Deutsche Forschungsgemeinschaft for support.

REFERENCES

- (1) Kelzenberg, S.; Eisenreich, N.; Eckl, W.; Weiser, V. Modelling Nitromethane Combustion. *Propellants, Explos., Pyrotech.* **1999**, *24*, 189–194.
- (2) Boyer, E.; Kuo, K. K. Modeling of Nitromethane Flame Structure and Burning Behavior. *Proc. Combust. Inst.* **2007**, *31*, 2045–2053.
- (3) Bouyer, V.; Darbord, I.; Hervé, P.; Baudin, G.; Le Gallic, C.; Clément, F.; Chavent, G. Shock-To-Detonation Transition of Nitromethane: Time-Resolved Emission Spectroscopy Measurements. *Combust. Flame* **2006**, *144*, 139–150.

- (4) Winey, J. M.; Gupta, Y. M. UV-Visible Absorption Spectroscopy to Examine Shock-Induced Decomposition in Neat Nitromethane. *J. Phys. Chem. A* **1997**, *101*, 9333–9340.
- (5) Winey, J. M.; Gupta, Y. M. Shock-Induced Chemical Changes in Neat Nitromethane: Use of Time-Resolved Raman Spectroscopy. *J. Phys. Chem. B* **1997**, *101*, 10733–10743.
- (6) Zhang, Y.-X.; Bauer, S. H. Modeling the Decomposition of Nitromethane, Induced by Shock Heating. *J. Phys. Chem. B* **1997**, *101*, 8717–8726.
- (7) Zhang, Q.; Li, W.; Lin, D.-C.; He, N.; Duan, Y. Influence of Nitromethane Concentration on Ignition Energy and Explosion Parameters in Gaseous Nitromethane/Air Mixtures. *J. Hazard. Mater.* **2011**, *185*, 756–762.
- (8) Oxley, J. C. In *Theoretical and Computational Chemistry*; Politzer, P., Murray, J. S., Eds.; Elsevier: Amsterdam, 2003; Vol. 12, Part 1, pp 5–48.
- (9) Singh, R. P.; Verma, R. D.; Meshri, D. T.; Shreeve, J. n. M. Energetic Nitrogen-Rich Salts and Ionic Liquids. *Angew. Chem., Int. Ed.* **2006**, *45*, 3584–3601.
- (10) Kozak, G. D. Factors Augmenting the Detonability of Energetic Materials. *Propellants, Explos., Pyrotech.* **2005**, *30*, 291–297.
- (11) Adams, G. F.; Shaw, R. W., J. Chemical Reactions in Energetic Materials. *Annu. Rev. Phys. Chem.* **1992**, *43*, 311–340.
- (12) Sikder, A. K.; Sikder, N. A Review of Advanced High Performance, Insensitive and Thermally Stable Energetic Materials Emerging for Military and Space Applications. *J. Hazard. Mater.* **2004**, *112*, 1–15.
- (13) Badgular, D. M.; Talawar, M. B.; Asthana, S. N.; Mahulikar, P. P. Advances in Science and Technology of Modern Energetic Materials: An Overview. *J. Hazard. Mater.* **2008**, *151*, 289–305.
- (14) Bhattacharya, A.; Guo, Y.; Bernstein, E. R. Nonadiabatic Reaction of Energetic Molecules. *Acc. Chem. Res.* **2010**, *43*, 1476–1485.
- (15) Brill, T. B.; James, K. J. Kinetics and Mechanisms of Thermal Decomposition of Nitroaromatic Explosives. *Chem. Rev.* **1993**, *93*, 2667–2692.
- (16) Butler, L. J.; Krajnovich, D.; Lee, Y. T.; Ondrey, G. S.; Bersohn, R. The Photodissociation of Nitromethane at 193 nm. *J. Chem. Phys.* **1983**, *79*, 1708–1722.
- (17) Guo, Y. Q.; Bhattacharya, A.; Bernstein, E. R. Photodissociation Dynamics of Nitromethane at 226 and 271 nm at Both Nanosecond and Femtosecond Time Scales. *J. Phys. Chem. A* **2009**, *113*, 85–96.
- (18) Kohge, Y.; Hanada, T.; Sumida, M.; Yamasaki, K.; Kohguchi, H. Photodissociation Dynamics of Nitromethane at 213 nm Studied by Ion-Imaging. *Chem. Phys. Lett.* **2013**, *556*, 49–54.
- (19) Lao, K. Q.; Jensen, E.; Kash, P. W.; Butler, L. J. Polarized Emission Spectroscopy of Photodissociating Nitromethane at 200 and 218 nm. *J. Chem. Phys.* **1990**, *93*, 3958–3969.
- (20) Moss, D. B.; Trentelman, K. A.; Houston, P. L. 193 nm Photodissociation Dynamics of Nitromethane. *J. Chem. Phys.* **1992**, *96*, 237–247.
- (21) Dey, A.; Fernando, R.; Abeysekera, C.; Homayoon, Z.; Bowman, J. M.; Suits, A. G. Photodissociation Dynamics of Nitromethane and Methyl Nitrite by Infrared Multiphoton Dissociation Imaging with Quasiclassical Trajectory Calculations: Signatures of the Roaming Pathway. *J. Chem. Phys.* **2014**, *140*, 054305.
- (22) Rockney, B. H.; Grant, E. R. Resonant Multiphoton Ionization Detection of the NO₂ Fragment from Infrared Multiphoton Dissociation of CH₃NO₂. *Chem. Phys. Lett.* **1981**, *79*, 15–18.
- (23) Rockney, B. H.; Grant, E. R. Detection of Photofragments by Multiphoton Ionization with Direct Resolution of Angular and Time-Of-Flight Distributions. *J. Chem. Phys.* **1982**, *77*, 4257–4259.
- (24) Homayoon, Z.; Bowman, J. M. Quasiclassical Trajectory Study of CH₃NO₂ Decomposition via Roaming Mediated Isomerization Using a Global Potential Energy Surface. *J. Phys. Chem. A* **2013**, *117*, 11665–11672.
- (25) Homayoon, Z.; Bowman, J. M.; Dey, A.; Abeysekera, C.; Fernando, R.; Suits, A. G. Experimental and Theoretical Studies of Roaming Dynamics in the Unimolecular Dissociation of CH₃NO₂ to CH₃O + NO. *Z. Phys. Chem. (Muenchen, Ger.)* **2013**, *227*, 1267–1280.
- (26) Zhu, R. S.; Lin, M. C. CH₃NO₂ Decomposition/Isomerization Mechanism And Product Branching Ratios: An Ab Initio Chemical Kinetic Study. *Chem. Phys. Lett.* **2009**, *478*, 11–16.
- (27) Zhu, R. S.; Raghunath, P.; Lin, M. C. Effect of Roaming Transition States upon Product Branching in the Thermal Decomposition of CH₃NO₂. *J. Phys. Chem. A* **2013**, *117*, 7308–7313.
- (28) Arenas, J. F.; Centeno, S. P.; López-Tocón, I.; Peláez, D.; Soto, J. DFT and CASPT2 Study of Two Thermal Reactions of Nitromethane: C–N Bond Cleavage and Nitro-To-Nitrite Isomerization. An Example of the Inverse Symmetry Breaking Deficiency in Density Functional Calculations of an Homolytic Dissociation. *J. Mol. Struct.: THEOCHEM* **2003**, *630*, 17–23.
- (29) McKee, M. L. Ab Initio Study of Rearrangements on the Nitromethane Potential Energy Surface. *J. Am. Chem. Soc.* **1986**, *108*, 5784–5792.
- (30) Bielski, B. H. J.; Timmons, R. B. Electron Paramagnetic Resonance Study of the Photolysis of Nitromethane, Methyl Nitrite, and Tetranitromethane at 77 K. *J. Phys. Chem.* **1964**, *68*, 347–352.
- (31) Rebbert, R. E.; Slagg, N. Primary Processes in the Photochemical Decomposition of Nitroalkanes. *Bull. Soc. Chim. Belg.* **1962**, *71*, 709–721.
- (32) Brown, H. W.; Pimentel, G. C. Photolysis of Nitromethane and of Methyl Nitrite in an Argon Matrix; Infrared Detection of Nitroxyl, HNO. *J. Chem. Phys.* **1958**, *29*, 883–888.
- (33) Jacox, M. E. Photodecomposition of Nitromethane Trapped in Solid Argon. *J. Phys. Chem.* **1984**, *88*, 3373–3379.
- (34) Kuznetsov, N. M.; Petrov, Y. P.; Turetskii, S. V. Kinetics of NO₂ Formation upon the Decomposition of Nitromethane Behind Shock Waves and the Possibility of Nitromethane Isomerization in the Course of the Reaction. *Kinet. Catal.* **2012**, *53*, 1–12.
- (35) Nicholson, A. J. C. Photolysis of Nitromethane. *Nature* **1961**, *190*, 143–144.
- (36) Guo, F.; Cheng, X.-l.; Zhang, H. Reactive Molecular Dynamics Simulation of Solid Nitromethane Impact on (010) Surfaces Induced and Nonimpact Thermal Decomposition. *J. Phys. Chem. A* **2012**, *116*, 3514–3520.
- (37) Han, S.-p.; van Duin, A. C. T.; Goddard, W. A.; Strachan, A. Thermal Decomposition of Condensed-Phase Nitromethane from Molecular Dynamics from ReaxFF Reactive Dynamics. *J. Phys. Chem. B* **2011**, *115*, 6534–6540.
- (38) Citroni, M.; Bini, R.; Pagliai, M.; Cardini, G.; Schettino, V. Nitromethane Decomposition under High Static Pressure. *J. Phys. Chem. B* **2010**, *114*, 9420–9428.
- (39) Kaiser, R. I.; Maksyutenko, P. A Mechanistical Study on Non-Equilibrium Reaction Pathways in Solid Nitromethane (CH₃NO₂) and D₃-nitromethane (CD₃NO₂) upon Interaction With Ionizing Radiation. *Chem. Phys. Lett.* **2015**, *631–632*, 59–65.
- (40) Kaiser, R. I.; Maksyutenko, P. Novel Reaction Mechanisms Pathways in the Electron Induced Decomposition of Solid Nitromethane (CH₃NO₂) and D₃-Nitromethane (CD₃NO₂). *J. Phys. Chem. C* **2015**, *119*, 14653–14668.
- (41) Maksyutenko, P.; Muzangwa, L. G.; Jones, B. M.; Kaiser, R. I. Lyman α Photolysis of Solid Nitromethane (CH₃NO₂) and D₃-Nitromethane (CD₃NO₂) - Untangling the Reaction Mechanisms Involved in the Decomposition of Model Energetic Materials. *Phys. Chem. Chem. Phys.* **2015**, *17*, 7514–7527.
- (42) Sato, T.; Narazaki, A.; Kawaguchi, Y.; Niino, H.; Bucher, G.; Grote, D.; Wolff, J. J.; Wenk, H. H.; Sander, W. Generation and Photoreactions of 2,4,6-Trinitrenol-1,3,5-triazine, a Septet Trinitrene. *J. Am. Chem. Soc.* **2004**, *126*, 7846–7852.
- (43) Stoll, S.; Schweiger, A. EasySpin, A Comprehensive Software Package for Spectral Simulation and Analysis in EPR. *J. Magn. Reson.* **2006**, *178*, 42–55.
- (44) Yamada, T.; Komaguchi, K.; Shiotani, M.; Benetis, N. P.; Sørnes, A. R. High-Resolution EPR and Quantum Effects on CH₃, CH₂D, CHD₂, and CD₃ Radicals under Argon Matrix Isolation Conditions. *J. Phys. Chem. A* **1999**, *103*, 4823–4829.

- (45) Takada, T.; Tachikawa, H. Hybrid DFT Study of the Hyperfine Coupling Constants of Methyl Radicals in Model Matrix Lattices. *Int. J. Quantum Chem.* **2005**, *105*, 79–83.
- (46) Dmitriev, Y. A. EPR Spectra of Deuterated Methyl Radicals Trapped in Low Temperature Matrices. *Low Temp. Phys.* **2005**, *31*, 423–428.
- (47) Shiga, T.; Lund, A. g Factor and Hyperfine Coupling Anisotropy in the Electron Spin Resonance Spectra of Methyl-, Ethyl-, and Allyl-Type Radicals Adsorbed on Silica Gel. *J. Phys. Chem.* **1973**, *77*, 453–455.
- (48) Morehouse, R. L.; Christiansen, J. J.; Gordy, W. ESR of Free Radicals Trapped in Inert Matrices at Low Temperature: CH₃, SiH₃, GeH₃, and SnH₃. *J. Chem. Phys.* **1966**, *45*, 1751–1758.
- (49) Dmitriev, Y. A.; Zhitnikov, R. A. EPR Study of Methyl Radicals. Anisotropy and Tumbling Motion in Low-Temperature Matrices. *J. Low Temp. Phys.* **2001**, *122*, 163–170.
- (50) Zhitnikov, R. A.; Dmitriev, Y. A. Detection of Free Radicals in Low-Temperature Gas-Grain Reactions of Astrophysical Interest. *Astron. Astrophys.* **2002**, *386*, 1129–1138.
- (51) Benetis, N. P.; Dmitriev, Y.; Mocci, F.; Laaksonen, A. Rotation Dynamics Do Not Determine the Unexpected Isotropy of Methyl Radical EPR Spectra. *J. Phys. Chem. A* **2015**, *119*, 9385–9404.
- (52) Chachaty, C.; Rosilio, C. Electron Paramagnetic Resonance Spectra of Radicals Formed by the Radiolysis of Solid Nitroalkanes. *J. Chim. Phys. Phys.-Chim. Biol.* **1967**, *64*, 777–790.
- (53) Chachaty, C. Investigation of the Free Radicals Obtained by α -Irradiation of Nitromethane at 77 K by Electron Paramagnetic Resonance. *J. Chim. Phys. Phys.-Chim. Biol.* **1965**, *62*, 827–831.
- (54) Symons, M. C. R. Redox Processes in Rigid Matrices with Specific Reference to Irradiated Nitromethane. *Faraday Discuss. Chem. Soc.* **1988**, *86*, 99–111.
- (55) McDowell, C. A.; Farmer, J. B.; Gardner, C. L.; Gerry, M. C. L.; Raghunathan, P. Electron Spin Resonance of Free Radicals Prepared by the Reactions of Methylene. Deuteriomethyl and Formaldiminoxy Radicals. *J. Phys. Chem.* **1971**, *75*, 2448–2452.
- (56) Jaszewski, A. R.; Jezierska, J. An Ab Initio Approach to the Structure and EPR Parameters of Formaldiminoxy Radical. *Chem. Phys. Lett.* **2001**, *334*, 136–144.
- (57) Chachaty, C.; Forchioni, A. Electron Paramagnetic Resonance Spectrum of the Methoxy Radical (CH₃O) in the Solid Phase. *C. R. Seances Acad. Sci., Ser. C* **1969**, *268*, 300–302.
- (58) Schaafsma, T. J.; Kommandeur, J. Electron Spin Resonance of NO₂. *Mol. Phys.* **1968**, *14*, 517–523.
- (59) Murphy, D. M. EPR (Electron Paramagnetic Resonance) Spectroscopy of Polycrystalline Oxide Systems. In *Metal Oxide Catalysis*; Wiley-VCH Verlag GmbH & Co. KGaA: Weinheim, Germany, 2009; pp 1–50.
- (60) Schwartz, R. N.; Clark, M. D.; Chamulitrat, W.; Kevan, L. Electron-spin resonance of NO₂ trapped in SiO₂ thin solid films. *J. Appl. Phys.* **1986**, *59*, 3231–3234.
- (61) Bielski, B. H. J.; Freeman, J. J.; Gebicki, J. M. Electron Spin Resonance of Nitrogen Dioxide in Frozen Solutions. *J. Phys. Chem.* **1968**, *72*, 1721–1725.
- (62) Shiotani, M.; Freed, J. H. ESR Studies of Nitrogen Dioxide Adsorbed on Surfaces. Analysis of Motional Dynamics. *J. Phys. Chem.* **1981**, *85*, 3873–3883.
- (63) Kasai, P. H.; Weltner, W.; Whipple, E. B. Orientation of NO₂ and Other Molecules in Neon Matrices at 4 K. *J. Chem. Phys.* **1965**, *42*, 1120–1121.
- (64) Pace, M. D. EPR Spectra of Photochemical Nitrogen Dioxide Formation in Monocyclic Nitramines and Hexanitrohexaazaisowurtzitanes. *J. Phys. Chem.* **1991**, *95*, 5858–5864.
- (65) Burch, D. S.; Tanttila, W. H.; Mizushima, M. X-band ESR Spectrum Of Nitrogen Dioxide. *J. Chem. Phys.* **1974**, *61*, 1607–1612.
- (66) Lunsford, J. H. EPR Spectra of Radicals Formed When NO₂ is Adsorbed on Magnesium Oxide. *J. Colloid Interface Sci.* **1968**, *26*, 355–360.
- (67) Stefan, S.; Schweiger, A. In *ESR Spectroscopy in Membrane Biophysics*; Springer: New York, 2007; Vol. 27, pp 299–321.
- (68) Jinguji, M.; Ohokubo, Y.; Tanaka, I. High Resolution EPR Spectrum of Nitric Oxide in the Gas Phase. *Chem. Phys. Lett.* **1978**, *54*, 136–138.
- (69) Yahiro, H.; Lund, A.; Shiotani, M. Nitric Oxide Adsorbed On Zeolites: EPR Studies. *Spectrochim. Acta, Part A* **2004**, *60*, 1267–1278.
- (70) Yahiro, H.; Kurohagi, K.; Okada, G.; Itagaki, Y.; Shiotani, M.; Lund, A. EPR Study on NO Introduced into Lithium Ion-Exchanged LTA Zeolites. *Phys. Chem. Chem. Phys.* **2002**, *4*, 4255–4259.
- (71) McConnell, A. A.; Mitchell, S.; Porte, A. L.; Roberts, J. S.; Thomson, C. Electron Paramagnetic Resonance Studies of Nitroxide Radicals Obtained from Caryophyllene Nitrosite. *J. Chem. Soc. B* **1970**, 833–838.
- (72) Tsuchiya, K.; Takasugi, M.; Minakuchi, K.; Fukuzawa, K. Sensitive Quantitation of Nitric Oxide by EPR Spectroscopy. *Free Radical Biol. Med.* **1996**, *21*, 733–7.
- (73) Rawson, E. B.; Beringer, R. Atomic Oxygen g-Factors. *Phys. Rev.* **1952**, *88*, 677–678.
- (74) Krongelb, S.; Strandberg, M. W. P. Use of Paramagnetic-Resonance Techniques in the Study of Atomic Oxygen Recombinations. *J. Chem. Phys.* **1959**, *31*, 1196–1210.
- (75) Barth, C. A.; Hildebrandt, A. F.; Patapoff, M. Atomic Oxygen and Nitrogen Density Measurements with EPR. *Discuss. Faraday Soc.* **1962**, *33*, 162–172.
- (76) Stoll, S.; Ozarowski, A.; Britt, R. D.; Angerhofer, A. Atomic Hydrogen as High-Precision Field Standard for High-Field EPR. *J. Magn. Reson.* **2010**, *207*, 158–63.
- (77) Dilger, H.; Roduner, E.; Scheuermann, R.; Major, J.; Schefzik, M.; Stößer, R.; Päch, M.; Fleming, D. G. Mass and Temperature Effects on the Hyperfine Coupling of Atomic Hydrogen Isotopes in Cages. *Phys. B* **2000**, *289–290*, 482–486.
- (78) Jen, C. K.; Foner, S. N.; Cochran, E. L.; Bowers, V. A. Electron Spin Resonance of Atomic and Molecular Free Radicals Trapped at Liquid Helium Temperature. *Phys. Rev.* **1958**, *112*, 1169–1182.
- (79) Karshenboim, S. G. Precision Physics of Simple Atoms: QED Tests, Nuclear Structure and Fundamental Constants. *Phys. Rep.* **2005**, *422*, 1–63.
- (80) Tiedeman, J. S.; Robinson, H. G. Determination of $g_j(^1\text{H}, I^2\text{S}_{1/2})/g_s(e)$: Test of Mass-Independent Corrections. *Phys. Rev. Lett.* **1977**, *39*, 602–604.
- (81) Anderson, L. W.; Pipkin, F. M.; Baird, J. C. Precision Determination of the Hyperfine Structure of the Ground State of Atomic Hydrogen, Deuterium, and Tritium. *Phys. Rev. Lett.* **1960**, *4*, 69–71.
- (82) Nagakura, S. Ultraviolet Absorption Spectra and π -electron Structures of Nitromethane and Nitromethyl Anion. *Mol. Phys.* **1960**, *3*, 152–62.
- (83) Bayliss, N. S.; McRae, E. G. Solvent Effects in the Spectra of Acetone, Crotonaldehyde, Nitromethane and Nitrobenzene. *J. Phys. Chem.* **1954**, *58*, 1006–1011.
- (84) Rabalais, J. W. Photoelectron Spectroscopic Investigation of the Electronic Structure of Nitromethane and Nitrobenzene. *J. Chem. Phys.* **1972**, *57*, 960–967.
- (85) Flicker, W. M.; Mosher, O. A.; Kuppermann, A. Variable Angle Electron-Impact Excitation Of Nitromethane. *J. Chem. Phys.* **1980**, *72*, 2788–2794.